Incoherent scatter Faraday rotation measurements on a radar with single linear polarization

Boris G. Shpynev

Institute of Solar-Terrestrial Physics, Irkutsk, Russia

Received 27 August 2001; revised 21 September 2003; accepted 25 March 2004; published 11 May 2004.

[1] This paper outlines an application of the incoherent scatter technique to the Irkutsk (Russia) VHF radar system, which has an antenna with a single, strictly linear polarization. Owing to ionospheric Faraday rotation, determination of wave plane polarization angle is essential to obtain electron density. We describe a new technique for electron density determination on a radar with single polarization based on the radar equation. This technique does not require additional external density calibration using other instruments such as ionosondes. *INDEX TERMS:* 6934 Radio Science: Ionospheric propagation (2487); 6952 Radio Science: Radar atmospheric physics; 6964 Radio Science: Radio wave propagation; *KEYWORDS:* ionospheric propagation, radar atmospheric physics, radio wave propagation

Citation: Shpynev, B. G. (2004), Incoherent scatter Faraday rotation measurements on a radar with single linear polarization, *Radio Sci.*, *39*, RS3001, doi:10.1029/2001RS002523.

1. Introduction

[2] The incoherent scatter (IS) method has existed for over four decades; a basic review can be found in *Evans* [1969, and references therein]. Several IS radars are currently active worldwide, and all of them are unique in design, frequency range, and specific signal processing/data acquisition techniques. The VHF radar system operated by the Institute of Solar-Terrestrial Physics in Irkutsk, Russia is no exception. Since the facility was designed for military radar purposes, a distinctive feature is its antenna design, which allows for transmission and reception of only one linear polarization. This system characteristic means that the signal at the radar receiver input undergoes quasi-periodic fading, caused by Faraday rotation. Although the polarization plane rotation feature can be used for calculation of absolute electron density, the single polarization channel leads to distortion of the IS spectrum or equivalently the correlation function of the received signal, and so the analysis is complicated.

[3] The concept of using the Faraday effect for estimation of N_e in incoherent scatter was first described by *Millman et al.* [1961]. In a later work [*Millman et al.*, 1964] the first measurements of the polarization plane angle of an IS signal, received on mutually orthogonal linearly polarized antennas, is described. The work of *Farley et al.* [1967] and *Farley* [1969] utilizes for Faraday measurements two coherent pulses transmitted with opposite circular polarizations, with receivers for each of the two component circular polarizations allowing the measurement of the phase difference between channels. For the Jicamarca radar, with a 50 MHz operating frequency, such a technique has proved optimal. The work of *Pingree* [1990] implemented this technique successfully for regular measurements, and the method (with subsequent data processing improvements) is now standard at Jicamarca.

[4] Faraday measurements have also been carried out at a 150 MHz radar in Kharkov (Ukraine) [*Tkachev and Rozumenko*, 1972]. The wave polarization plane at the Kharkov center frequency makes a smaller number of revolutions than at Jicamarca. Since the separately measured polarization channels at Kharkov are not completely independent due to crosstalk effects, *Grigorenko* [1979] developed a method of N_e definition using an analysis of power profile extreme points. The method works only at F2 layer heights with high electron density in daytime. If the electron density is low, usually there are not enough extreme points for restoration of N_e structure with acceptable height resolution.

[5] At Irkutsk, the radar center frequency is at 154–162 MHz and radar can radiate and receive only one linear polarization. However, unlike Kharkov, the Irkutsk antenna system has a polarizing filter, reducing the orthogonal polarization level by 30 dB. Therefore it is feasible to assume that signal polarization on both transmission and reception is strictly linear. This allows to obtain an exact equation for the received signal and so

0048-6604/04/2001RS002523$11.00

give us a solution which relates it directly to N_e. In the present work, we derive this technique on the basis of the radar equation.

2. Incoherent Scatter Measurement Radar Equation Accounting for Faraday Effects

[6] The radar equation can be obtained for the IS method, accounting for Faraday effects, on the basis of the statistical theory of scattering [*Tatarsky*, 1967; *Rytov et al.*, 1978]. For antennas with circular polarization, such an equation can be found in *Suni et al.* [1989] with main techniques developed by *Kravtsov and Orlov* [1980]. The derivation of the equations are complex, and so we only specify the basic differences from the circular polarization case before carrying out the analysis of final expressions. For a derivation of the radar equation we follow an expression from *Suni et al.* [1989]:

$$U_a(t) = \sqrt{\frac{P}{4\pi}} r_e e^{j(\beta-\omega_0 t)} \int \frac{dr}{r^2} D_{tra}(\overrightarrow{l_r}) D_{rec}(\overrightarrow{l_r}) p \cdot \delta N\left(t-\frac{r}{c}, r\right) a\left(t-\frac{2r}{c}\right) e^{i2k_0 r} \quad (1)$$

Here $U_a(t)$ is the complex envelope of the received signal, P is the peak transmitted power, r_e is the classical electron radius, β is the initial transmitted wave phase, ω_0 is the transmitter frequency, $k_0 = \omega_0/c$, $\vec{l}_r = \vec{r}/r$, $p = (\vec{l}_{rec} \cdot [\vec{l}_r \times [\vec{l}_r \times \vec{l}_{tra}]])$ is the polarization multiplier, $\vec{l}_{tra,rec}$ are the individual vectors of polarization, $\vec{D}_{tra,rec}$ are the normalized antenna patterns for transmission and reception, δN are the electron density fluctuations, and $a(t)$ is the complex envelope of the transmitted signal.

[7] To account for antenna linear polarization, we replace the wave function $e^{i2_0 r}$ with a sum of geometrical optic expressions for ordinary and extraordinary waves:

$$e^{i2k_0 r} \Rightarrow {}^1\!/_2\left(e^{i2k_0\varphi_o} + e^{i2k_0\varphi_x}\right) \quad (2)$$

where

$$\varphi_{o,x}(r) = \int_0^{\vec{r}} n_{o,x} d\sigma \cong \int_0^{\vec{r}} n d\sigma \pm \frac{1}{2}\int_0^{\vec{r}} v\sqrt{u}\cos\alpha \cdot d\sigma = \varphi(r) \pm \frac{1}{2}\phi(r) \quad (3)$$

are eikonals of ordinary and extraordinary waves [*Kravtsov and Orlov*, 1980], $n_{o,x}$ is the index of refraction, $v = \frac{\omega_p^2}{\omega_0^2}$, $u = \frac{\omega_H^2}{\omega_0^2}$, $\omega_p^2 = \frac{N_e e^2}{\varepsilon_0 m_e}$, $\omega_H = \frac{e|\vec{B}|}{m_e}$. Here N_e is the electron density, e is the electron charge, m_e is the electron mass, ε_0 is the permittivity of free space, $\vec{B}$ is the magnetic fied, α is the angle between $\vec{B}$ and $\vec{k}_0$, and the integrals are carried out along the appropriate beams. Substituting (3) in (2), we have for the wave function:

$$e^{i2k_0 r} \Rightarrow e^{i2k_0\varphi(\vec{r})}\left(e^{ik_0\phi(\vec{r})} + e^{-ik_0\phi(\vec{r})}\right)/2 = e^{i2k_0\varphi(\vec{r})}\cos\Omega(r)\Omega(r) = k_0\phi(r) \quad (4)$$

The variable $\Omega(r)$ is the rotation angle of rotating of the polarization plane from its initial position on the ground to current range along the path of wave propagation. Next we substitute (4) in (1) and consider the expressions for average spectral density $S(\omega, \tau) = \langle|U(\omega, \tau)|^2\rangle$, where τ is the delay from beginning of emission. Integration of the waves in the far-field range of a monostatic transmitting/receiving radar antenna give us the opportunity to express the influence of the antenna geometry through antenna gain G. This results in the radar equation, which connects the spectrum of the received signal with the spectrum of plasma fluctuations $\rho(r, \omega)$. This equation has been derived by many authors [e.g., *Sheffield*, 1975]. If we also assume that $\rho(r, \omega)$ is constant inside the spatial volume occupied by transmitted pulse, then for spectral density we have

$$S(\omega,\tau) = A\int d\nu \cdot \tilde{\rho}(\nu) F(\omega-\nu,\tau) \quad (5)$$

$$F(\omega,\tau) = \int \frac{dr}{r^2} W(\omega,r,\tau)\cdot\cos^2(\Omega(r)) \quad (6)$$

$$W = \frac{1}{(2\pi)^2}\int dt_1 dt_2 O(t_1-\tau) O^*(t_2 - a\left(t_1 - \frac{2r}{c}\right) a^* \cdot (t_2-\tau)\frac{2r}{c}) \cdot e^{i(\omega-\nu)(t_1-t_2)} \quad (7)$$

$$A = PG/k_0^2 \quad (8)$$

In (5)–(7) ν, t_1 and t_2 are the integration variables. Function $O(t-\tau)$ determines the delay and the shape of the signal analysis window, which usually is rectangular and it length is equal to sounding pulse duration. The integration of (5) on ω gives the total power of the signal, scattered by the plasma volume, the form and relative weight of which is defined by function (6), which can be called the modified ambiguity function. Total scattering cross section of plasma for wavelength $\sim 2m$ has the well known expression [*Buneman*, 1962]:

$$\rho_0 = \rho(r, t=0) = \pi r_e^2 \frac{N_e(r)}{1 + T_e(r)/T_i(r)} \quad (9)$$

So far as we are interested in power from a fixed range only, the window $O(t-\tau)$ becomes a delta function in

time, and by using (9), the power of the incoherent scattered signal can be expressed as

$$P(\tau) = \pi r_e^2 A \int \frac{dr}{r^2} \frac{N_e(r)\cos^2(\Omega(r))}{(1 + T_e(r)/T_i(r))} \left| a\left(\tau - \frac{2r}{c}\right)\right|^2 \tag{10}$$

The equations (5)–(10) are the required radar equations, which can be used for derivation of ionospheric plasma parameters through fitting to the functions $S(\omega, \tau)$ and $P(\tau)$. The difference of these equations from traditional ones is the presence of Faraday rotation multiplier $\cos^2(\Omega(r))$, in the expression for power, and in the modified ambiguity function (6). When spectral power density $S(\omega, \tau)$ is measured experimentally (Figure 1), the Faraday effect causes a range modulation, which is visible as two minima near 450 and 575 km. To obtain necessary spectral power estimates, a long transmitted pulse of 750–800 μs is used. At this mode, which we call as "long pulse mode", the measured minima of power always exceed zero level under integration over the scattering volume. The fast variations near the ionosphere electron density maximum at 300–400 km are not visible at all. Comparing to traditional fitting technique the present one needs the calculation of the ambiguity function separately for all heights. In the other detail the processing of spectra does not differ from traditional, and was repeatedly tested at joint Irkutsk - Millestone Hill observations.

[8] To take the Faraday effect account for fitting of experimental spectra and getting electron density itself we must provide an independent way to derive the value of $\Omega(r)$. This can be done by using the expressions (10), providing a short transmitted pulse is used (short pulse mode). If the value of $\Omega(r)$ is obtained, we can simultaneously fit the IS spectra and determine the $N_e(r)$ profile by using the well known expression [*Ginzburg*, 1967]:

$$\Omega(\vec{r}) = \frac{e^3 B_0 \cos\alpha}{2\varepsilon_0 m_e^2 \omega_0^2 c} \int_0^{\vec{r}} N_e(z)dz \tag{11}$$

from which we can obtain $N_e(r) \approx \frac{d\Omega(r)}{dr}$. Here we assumed that the intensity of magnetic field $B_0 = |\vec{B}|$ is given and constant inside the range of measurements. Hence, the key task of incoherent scatter measurements on an antenna with single linear polarization is the solving of the equation (10) relative to $N_e(r)$.

3. Determination of Electron Density

[9] To analyze the properties of equation (10) we write it in the following form:

$$P(\tau) = \int \tilde{P}(r) \left| a\left(\tau - \frac{2r}{c}\right)\right|^2 dr, \tag{12}$$

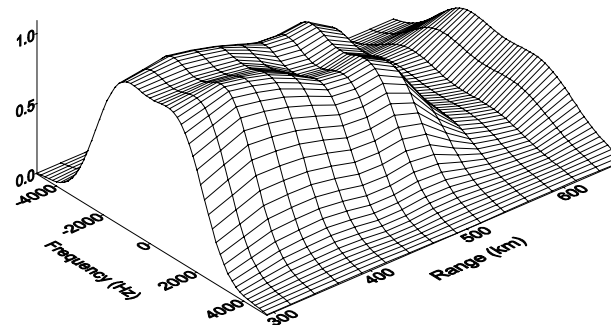

Figure 1. Example of the altitude distribution of experimental power spectra measured by long pulse $T = 750$ μs. The variation of spectral power with altitude on this plot is caused by Faraday effects.

$$\tilde{P}(r) = \pi r_e^2 A \frac{N_e(r)\cos^2(\Omega(r))}{r^2(1 + T_e(r)/T_i(r))} \tag{13}$$

From (12) and (13) we can see that there are two basic issues for determination of $N_e(r)$. The first issue is the convolution of the experimental power profile with the characteristics of the transmitted pulse. Additionally, there is a nonlinear dependence $\tilde{P}(r)$ on $N_e(r)$, which enters in (13) as a multiplier and stands under the integral sign in expression (11). Fortunately, the nonlinear connection between $\tilde{P}(r)$ and $N_e(r)$ is not the basic problem of the given technique, since if we replace variables by using the equation

$$N_e(r) = \frac{1}{\gamma}\frac{d\Omega}{dr} \tag{14}$$

where

$$\gamma = \frac{e^3 B_0 \cos\alpha}{2\varepsilon_0 m_e^2 \omega^2 c} \tag{15}$$

then we reduce the equation (13) to a coupled differential equation. Solving this system gives us:

$$\frac{1}{A_0}\int_0^r \tilde{P}(r') \cdot r'^2 \cdot (1 + Te(r')/Ti(r'))dr' = \Omega + \frac{\sin(2\Omega)}{2} + C \tag{16}$$

where $A_0 = A\pi r_e^2/2\gamma$, and the constant $C = 0$ as $\Omega(r = 0) = 0$. As the expression under the integral sign in (16) is always positive then by measuring the function $\tilde{P}(r)$, and using known expressions for A_0 and the ratio T_e/T_i we can solve numerically (16) and to determine the value of $\Omega(r)$.

[10] Removing effects of convolution with the transmitted pulse is a more difficult task. The first problem is

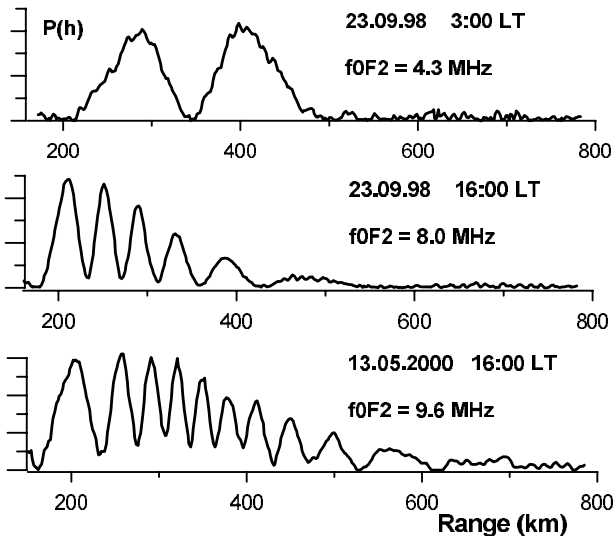

Figure 2. Examples of short pulse power profiles, corresponding to different ionospheric conditions. (top) Nighttime conditions with low electron density and 200 μs sounding pulse. (middle and bottom) Daytime conditions with different electron density, 100 μs and 50 μs sounding pulses, respectively.

that for power measurements it is impossible to use the same transmitted pulse (750–800 μs) as for spectral measurements, since at the electron density peak the effect of convolution completely hides the Faraday effect. Secondly, we cannot use very short pulses, the convolution with which can be neglected, because they have insufficient energy for measurements at large heights. Therefore, for optimal measurements we must use pulses which are long enough to supply necessary energy, but which are short enough to allow us remove the convolution expressed in (12). This ''short pulse mode'' goes just after ''long pulse mode'' and uses another carried frequency. The design of transmitter's modulators on Irkutsk's radar gives us the opportunity to use the total length of emission not less then 850 μs, but ionospheric conditions sometimes need using such short sounding pulses at ''short pulse mode'' as 50 μs. To keep necessary total pulse length we change for such conditions to ''long pulse'' duration within (750–800 μs). In Figure 2, measurements of scattered power in relative units versus range are given for different ionospheric conditions. The top profile is measured at nighttime with a pulse of T = 200 μs duration, the middle one during day time with a T = 100 μs pulse, and the bottom one during high electron density conditions with T = 50 μs pulse. For better understanding of ionospheric conditions, corresponding f_0F2 frequencies are presented on the plots. The figure shows that the influence of convolution on the transmitted pulse is almost invisible on the top and middle panel of Figure 2 due to the long period of Faraday variations, but convolution effects clearly appear on the bottom panel as nonzero profile minima. As power profiles can be of different forms, the transmitted pulse duration must be changed flexibly during the experiment. Nevertheless, the measured power profiles demonstrate the necessity of deconvolution with the transmitted pulse shape.

4. Deconvolution of Power Profiles by Using the Transmitted Pulse Shape

[11] Deconvolution problems are frequently faced in remote sensing systems. They belong to a class of inverse theory problems which in general are difficult to realize in practice. We can express the convolution operation as

$$g(x) = \int f(y)k(x-y)dy \tag{17}$$

where the real function $f(x)$ is convolved with a kernel $k(x)$. The most general method of deconvolution is to perform transitions to frequency space, to divide the Fourier-space expression $f(\omega)$ by the Fourier-space expression $k(\omega)$, and finally return back to the variable x [*Natterer*, 1986]. However, the given approach has an essential problem in the divergence of the result near the zeroes of $k(\omega)$. To solve this contradiction we could employ complex regularization algorithms, which are often computationally intensive and very sensitive to experimental noise. However, for the present problem, there are features which allow simplification. For example, we can assert that the power profile is always positive definite. Also, we can specify that the transmitted pulse must have an almost rectangular shape. Using these features of our measurement technique, we have developed [*Voronov and Shpynev*, 1998] a deconvolution method which in practice is faster and more immune to experimental noise compared with traditional procedures. The method is based on the fact that each positive definite function can be approximated by the sum of horizontal rectangles $R_i(x)$ of identical height and various lengths (Figure 3b):

$$f(x) = \sum R_i(x) \tag{18}$$

It is clear that minimal splitting of the original function into rectangles must lead to better approximation. We consider our kernel $k(y)$ (the transmitted pulse) also to be rectangular with amplitude 1 and with duration τ_0, which is equal to duration of the transmitted pulse. As the convolution of a rectangle $R_i(x)$ with a rectangle $k(y)$ is a trapezoid $T_i(x)$ (Figure 3a) with equal slopes at front and

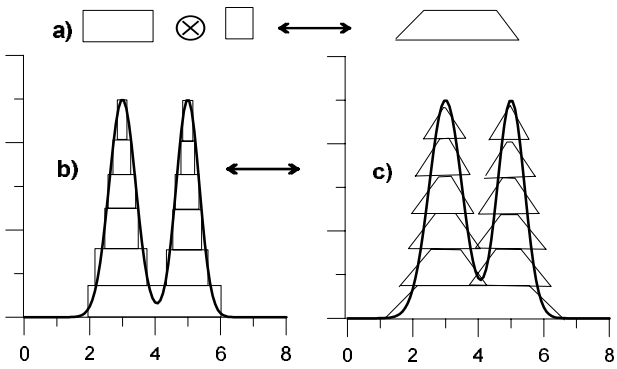

Figure 3. Illustration of approximation method for deconvolution. (a) Convolution of two rectangles; (b) approximation of positive definite functions by horizontal rectangles; (c) result of convolution as a sum of appropriate trapezoids.

back, with duration τ_0, the approximated equation of convolution has the form

$$g(x) = \sum T_i(x) \tag{19}$$

If we now reverse the task and approximate the convolution result by a sum of trapezoids $T_i(x)$ (Figure 3c), and replace each trapezoid by an appropriate rectangle, we obtain the required approximation for $f(x)$. Since the approximation of the positive function $g(x)$ by a sum of trapezoids is always possible, the given method is always stable, and experimental noise will influence only the accuracy of approximation. The method requires a minimal number of calculations and its accuracy depends fundamentally on the quality of approximation of the experimental power profile by trapezoids.

5. Practical Realization of $N_e(r)$ Derivation

[12] After the deconvolution of $P(r)$ and determination of $\tilde{P}(r)$, with known temperature ratio T_e/T_i and constant A_0 we can express the angle $\Omega(r)$ by using the equation (16) follows:

$$\frac{1}{A_0}\int_0^r \tilde{P}(r')\cdot r'^2\cdot(1+T_e(r')/T_i(r'))dr' \simeq \Omega + \frac{\sin(2W)}{2} \tag{20}$$

Here, the symbol $\simeq$ in (20) and beyond indicates the use of the approximate deconvolution algorithm. To determine in (20) the constant A_0, we assume $T_e/T_i = 1$. This condition is almost always true at night, and corresponds to the top diagram of Figure 2. In this case, the integral in the left part of (20) can be determined for all values of r from experimental data, and the absolute calibration of measurements can be carried out by using that the integral in the left part of (20) between two neighbor minima is equal to π. Then the constant A_0 can be determined from the condition:

$$A_0 \simeq \frac{2}{\pi}\int_{r_j}^{r_{j+1}} \tilde{P}(r)r^2dr \tag{21}$$

where r_j are the coordinates of points where complete fading occurs.

[13] If we begin measurements during daytime hours when $T_e/T_i \neq 1$, we can modify our technique to consider the T_e/T_i ratio as a constant inside an interval between neighbor minima, as can be seen in Figure 2 (middle and bottom plots). For this case, to obtain absolute calibration we define the set of normalizing constants A_0^j separately for every j-th interval. In this case we obtain

$$A_0^j \simeq \frac{1}{\pi}\int_{r_j}^{r_{j+1}} \tilde{P}(r)r^2dr \tag{22}$$

Of course, the constants A_0^j will differ from the actual constant A_0 at least by a factor of 2, but this does not affect our result since we are only interested in $N_e(r)$.

[14] If the constant A_0 is already determined, and the power profile has a sufficient number of polarization-induced minima (as in the middle and bottom diagrams of Figure 2), from (20) we can obtain an estimation of the T_e/T_i ratio itself. If we take into consideration the variations of the radar system constant versus the time, and fix the ratio T_e/T_i constant inside the intervals between neighbor minima of the profile $\tilde{P}(r)$, then for the j-th interval we have

$$(T_e/T_i)_j \simeq \frac{\pi A_0}{\int_{r_j}^{r_{j+1}} \tilde{P}(r)\cdot r^2dr} - 1 \tag{23}$$

This equation can be used both for processing of the IS spectra and for a more exact definition of $N_e(r)$. We should note that everywhere at $N_e(r)$ processing we need the T_e/T_i ratio (not T_e and T_i separately).

[15] During numerical processing of the equation (20) the solution becomes unstable in regions close to zeroes of a power profile. This happens both because the signal fades to the point where it is comparable to noise, and because of the nonlinear behavior of $\frac{sin(2\Omega)}{2}$ near the minima when small changes of integral in the left part of (20) correspond to large variations of the angle $\Omega(r)$. To avoid this instability, we instead use an approximation of the profiles near minima locations before calculation of $\Omega(r)$.

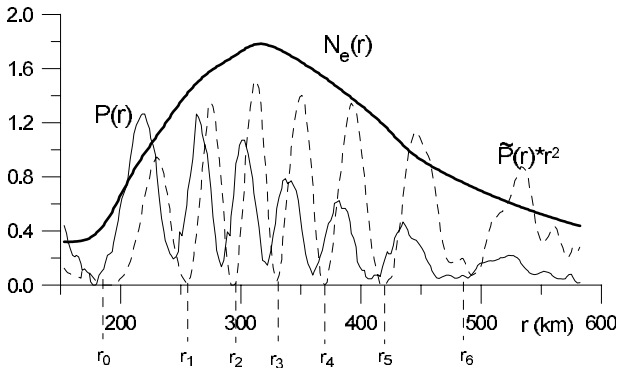

Figure 4. Processing of short pulse $T = 70$ μs power profiles (thin solid line). The first stage excludes convolution with the transmitted pulse and accounts for the factor r^2 (dashed line). The second stage solves the equation (20) and determines $N_e(h)$ (thick line). The shape of $N_e(h)$ is not proportional to envelope of $\tilde{P}(r)r^2$ due to different value of T_e/T_i ratio.

[16] The solution of the equation (10) can also be carried out by direct fitting of a specified profile shape to the entire profile $P(r)$, accounting for convolution with the transmitted pulse and for the Faraday effect. However, this kind of algorithm requires much more computing resources and is in many cases unacceptable for regular measurements. At the present time, we use a compromise algorithm in which the first approximation of $\Omega(r)$ is determined by solving the equation (20). Once this has been obtained, least squares fitting is used with the direct formula (10). This is very helpful at high altitudes, where owing to the r^2 factor the influence of noise is much more significant.

[17] Unfortunately, direct measurements of electron density in Irkutsk at heights lower than 160 kilometers are currently impossible owing to ground clutter. However, indirect information about E region conditions can be obtained on the basis of the value of total electron content, from the Earth's surface up to a height of 160 kilometers. These estimates are made possible since the height of the first polarization minimum in practice is always higher than 160 km. This information may be useful for analysis of E region variations during major geomagnetic storms.

6. Spatial Resolution and Measurement Accuracy

[18] Since during data processing we carry out deconvolution, formally (mathematically, in view of accuracy of deconvolution algorithm) the spatial resolution of $\tilde{P}(r)$ measurements is defined only by the sampling frequency. However, owing to noise and to the previously mentioned problem of algorithm instability near the profile zeroes, the same resolution for $N_e(r)$ cannot usually be achieved. It may be seen that there is no signal near the minima and there are no data here. However, in practical use, the positions of minima points are the data itself and, fortunately, the variation of $N_e(r)$ at heights of zeroes (above 200 km) are slow, and these data gaps are not critical if some approximation is used. As a best approximation, we select the spatial resolution which results using a transmitted pulse of duration 50–200 μs. Of cause, resolution will be better when $N_e(r)$ is larger and the transmitted pulse is shorter.

[19] Since the noise level also defines the accuracy of $N_e(r)$ derivation, for estimation of measurement error the following algorithm is used. The profile $N_e(r)$, obtained as a result of calculations, is substituted in expression (10), and the resulting power profile $P'(r)$ is compared with the experimental profile $P(r)$. Using a sliding window with a duration T, an average square-law deviation $\sigma^2(r_j) = \sum_{i=j}^{j+T} (P'(r_i) - P(r_i))^2$ is calculated at every height. The value of σ^2, expressed in percentage terms, is then used as the relative error of measurements. In this way, calculation errors appear in the value of measurement error, including errors near minima, from noise and other causes.

[20] An example of calculation results is shown in Figure 4, where the thin continuous line is an experimental power profile, the dotted line is the profile $\tilde{P}(r)$ after deconvolution and correction for the factor r^2, and the thick line is the restored shape of $N_e(r)$ after the algorithm has been applied. Curves are presented in relative units. The shape of $N_e(h)$ is not proportional to

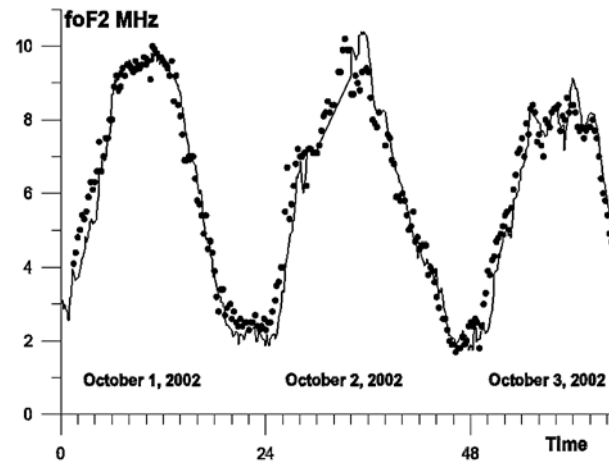

Figure 5. Comparison of critical frequencies derived by the described technique and by ionosonde. Continuous lines correspond to radar data with 6 minute resolution. Circles are ionosonde data with 15 minute resolution.

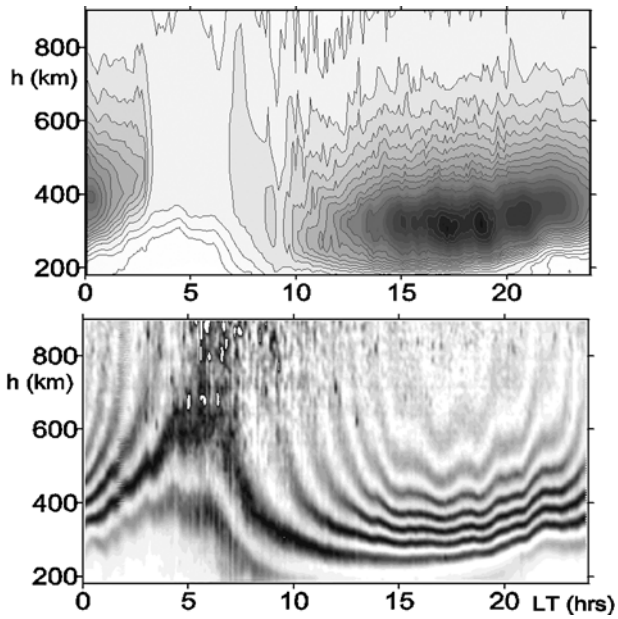

Figure 6. Example of data processing on April 14, 2001. (bottom) Normalized power profile, plotted as a function of time. (top) $N_e(h)$ profile. The black curves on the bottom panel are the rotational isopleths, which may be used for analysis of traveling ionospheric disturbances (TID). TIDs are visible as wavelike distortion of isopleths in the time interval 14–22 LT. TID height distribution and dynamics are also visible in variations of $N_e(h)$ (top panel).

envelope of $\tilde{P}(r)r^2$ due to different value of T_e/T_i ratio at different altitudes. The greater value of T_e/T_i, the less the area under power profile curve.

7. Testing and Applying the Method

[21] The described method of $N_e(r)$ calculation has been implemented for processing of regular experimental data measured at the Irkutsk incoherent scatter radar. For testing of the method, we have compared the critical frequency of the F2 ionosphere maximum, calculated from $N_e(h)$ profile, with f_0F2 data of an ionosonde located at Irkutsk which has resumed operations this year. The comparison is presented in Figure 5, where circles correspond to the ionosonde data with 15 minute time resolution, and continuous lines represent the radar data with 6 minutes resolution. As one can see from this plot, there is good agreement between the measured values, even for the daytime interval on October 3, when wavelike variations of f_0F2 are present. Some differences in the plots may be caused both by the different time resolution of methods and the slightly different separations of radar and ionosonde (approximately 120 km).

[22] To show the capabilities of our technique, in Figure 6 we present two contours, received on April 14, 2001. One of them (bottom panel) is the normalized power profile, plotted as a function of time, and another one (top panel) is the $N_e(h)$ profile result of our algorithm, plotted in the same manner. The black curves on the bottom panel are the rotational isopleths, which may be used for analysis of traveling ionospheric disturbances (TID) as in the work of *Goodman* [1971] for investigation of neutral internal and surface gravity waves. TIDs are visible in Figure 6 as wavelike distortions of isopleths in the time interval 14–22 LT. Time variations of $N_e(h)$ resulting from our algorithm (top panel of Figure 6) show not only changing electron density with time, but also indicate the heights where these variations appear and their dynamic behavior with altitude.

8. Conclusion

[23] We have described a method of $N_e(r)$ derivation, with account for Faraday effect, which allows us to use an antenna with a single linear polarization for ionospheric research. For realization of incoherent scatter measurements on such systems, we must carry out simultaneously two types of measurements: traditional measurements of the spectra (or correlation functions) using a long pulse, and additional measurements of power using a short pulse. These allow us to take into account ionospheric Faraday effects during processing and to obtain the absolute values of electron density without additional external calibration.

[24] **Acknowledgments.** The author is grateful to A. P. Potekhin, I. I. Orlov, O. I. Berngardt, A. L. Voronov, and P. J. Erickson for useful discussion and help with preparing the paper. This work was supported by grants of RFBR (Russian Foundation for Basic Research) NSh-272.2003.5 and 01-05-65374.

References

Buneman, O. (1962), Scattering of radiation by the fluctuations in a nonequilibrium plasma, *J. Geophys. Res.*, *67*, 2050–2053.

Evans, J. V. (1969), Theory and practice of ionosphere study by Thomson scatter radar, *Proc. IEEE*, *57*, 496–530.

Farley, D. T. (1969), Faraday rotation measurements using incoherent scatter, *Radio Sci.*, *4*(2), 143–152.

Farley, D. T., J. P. McClure, D. L. Sterling, and J. G. Green (1967), Temperature and composition of the equatorial ionosphere, *J. Geophys. Res.*, *72*, 5837.

Ginzburg, V. L. (1967), *Propagation of Electromagnetic Waves in a Plasma*, Nauka, Moscow.

Goodman, J. M. (1971), Traveling ionospheric disturbances observed through use of a Thomson scatter technique

employing Faraday rotation at 140 MHz, *J. Atmos. Terr. Phys.*, *33*, 1763–1777.

Grigorenko, E. B. (1979), *Ionos. Issled.*, *27*, 60–73.

Kravtsov, Y. A., and Y. I. Orlov (1980), *The Geometric Optics of Nonhomogeneous Media*, Nauka, Moscow.

Millman, G. H., et al. (1961), Effect of Faraday rotation on incoherent backscatter observations, *J. Geophys. Res.*, *66*, 1564–1568.

Millman, G. H., V. C. Pineo, and D. P. Hynek (1964), Ionospheric investigations by the Faraday rotation of incoherent backscatter, *J. Geophys. Res.*, *69*, 4051.

Natterer, F. (1986), *The Mathematics of Computerized Tomography*, John Wiley, Hoboken, N. J.

Pingree, J. E. (1990), Ph.D. thesis, Cornell Univ., Ithaca, N. Y.

Rytov, S. M., Y. A. Kravtsov, and V. I. Tatarsky (1978), *Introduction to Statistical Radio Physics*, Nauka, Moscow.

Sheffield, J. (1975), *Plasma Scattering of Electromagnetic Radiation*, Academic, San Diego, Calif.

Suni, A. L., V. D. Tereshchenko, E. D. Tereshchenko, and B. Z. Khudukon (1989), *Incoherent Scatter of Radio Waves in the High-Latitude Ionosphere*, 182 pp., AN SSSR, Apatity.

Tatarsky, V. I. (1967), *Wave Propagation in a Turbulent Atmosphere*, 548 pp., Nauka, Moscow.

Tkachev, G. N., and V. T. Rozumenko (1972), *Geomagn. Aeron*, *12*(4), 657–661.

Voronov, A. L., and B. G. Shpynev (1998), Excluding of convolution with sounding impulse in experimental Incoherent Scatter power profile, *Proc. SPIE*, *3583*, 414–418.

B. G. Shpynev, Institute of Solar-Terrestrial Physics, P.O. Box 4026, 664033 Irkutsk, Russia. (shpynev@iszf.irk.ru)